Impact of Changes in Resolution on a Multi-scale Modeling Framework with a Higher-order Turbulence Closure in its Cloud Resolving Model Component

Anning Cheng[1,2], and Kuan-Man Xu[1]

1. NASA Langley Research Center, 2. SSAI, Hampton, VA

1. Introduction

The representation of clouds, especially low-level clouds, is the largest source of uncertainty in climate simulations by general circulation models (GCMs). Low level clouds associated with turbulent circulations of small spatial scales (meters to kilometers) cannot be adequately resolved by the multiscale modeling framework (MMF) despite its successes in simulating phenomena associated with deep convective clouds (Khairoutdinov et al. 2008).

In an MMF a cloud resolving model (CRM) is embedded at each grid cell of the parent GCM to represent cloud physical processes. To better represent the sub-CRM-scale processes, a higher-order turbulence closure (HOC) was implemented in the MMF model to parameterize the turbulence and low-level clouds (Cheng and Xu 2011). The MMF results are expected to be sensitive to the resolution of both the CRM and the host GCM, especially the vertical resolution. In this study, we extensively investigate the dependence of climate simulation with an MMF model on resolution.

2. Experiment design

The MMFs used in this study consist of the Community Atmosphere Model (CAM3.5) and a 2D CRM embedded in each GCM atmospheric grid column. The CRM component of the MMF is the System for Atmospheric Modeling (SAM) with an intermediately-prognostic higher-order turbulence closure (IPHOC) scheme implemented. This MMF is hereafter referred to as SPCAM-IPHOC since the original MMF with the standard SAM is known as SPCAM.

Two sets of experiments were made: 1) A two year and three month simulation using SPCAM-IPHOC with the semi-Lagrangian T21 dynamic core; and 2) A four year simulation using SPCAM-IPHOC with finite-volume (fv-) 1.9°X2.5° dynamic core. The number of vertical levels is doubled for low levels (p > 700 hPa) compared with set 1 in order to better resolve boundary-layer clouds. The results from the last three years of the second set are used and denoted by SPCAM-IPHOC-hires, while those from the last two years of the first set are used in the following plots.

3. Motivation

Offline CRM tests show that doubling of resolution below 700 hPa results in more reasonable cloud evolution.

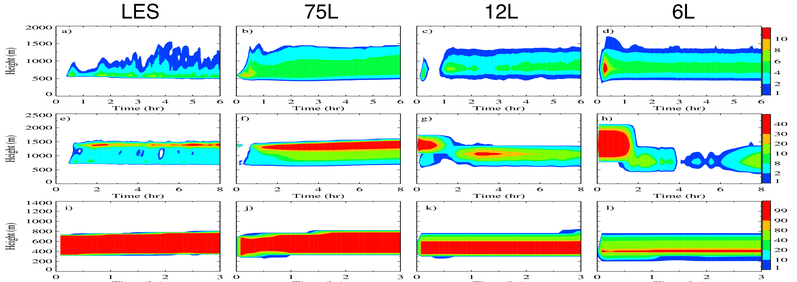

Fig. 1 Time-height cross section of cloud fraction evolution. The BOMEX shallow cumulus case is shown in the upper row, the ATEX shallow cumulus-to-stratocumulus transition case is shown in the middle, and the ASTEX stratocumulus case is in the bottom row, respectively.

4. Results

A 5% increase in global mean low cloud amount and better spatial distributions

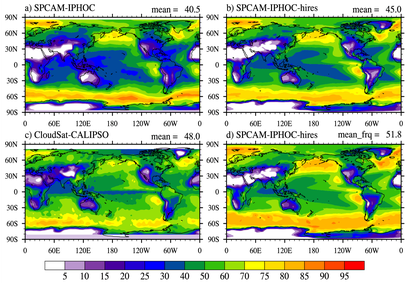

Fig. 2. Global distribution of annual mean low-level (p > 700 hPa) cloud amounts (%) from SPCAM-IPHOC (a), SPCAM-IPHOC-hires (b), and the CloudSat and CALIPSO observations (c), and the frequency of low cloud occurrence in a GCM box from SPCAM-IPHOC-hires (d).

More reasonable vertical structures

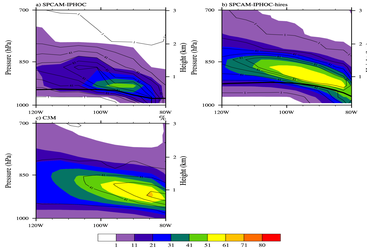

Fig. 3. Cross-sectional plots of annual-mean cloud fraction (%, shaded) and cloud liquid water (mg kg^{-1}, contoured) along 15°S over the southeast Pacific from SPCAM (a), SPCAM-IPHOC-hires (b) and C3M observations (c, CERES, CALIPSO, CloudSat and MODIS).

A 5% increase of global mean high cloud amount

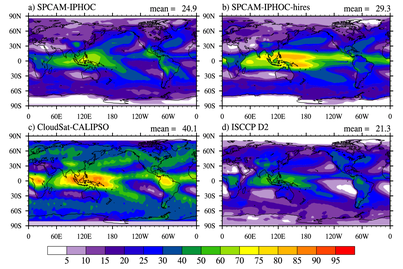

Fig. 4. Global distribution of annual mean high-level (p < 400 hPa) cloud amounts (%) from SPCAM-IPHOC (a), SPCAM-IPHOC-hires (b), and the CloudSat and CALIPSO observations (c), and the ISCCP-D2 (d).

Excessive precipitation near west Pacific disappears

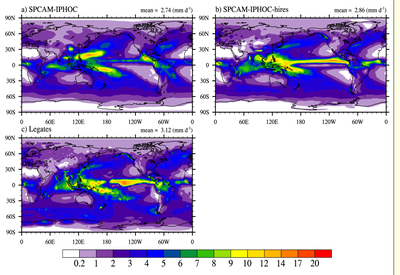

Fig. 5. Global distribution of annual mean surface precipitation from SPCAM (a), SPCAM-IPHOC-hires (b) and Legates and Willmott observations (c).

Larger surface latent heat flux

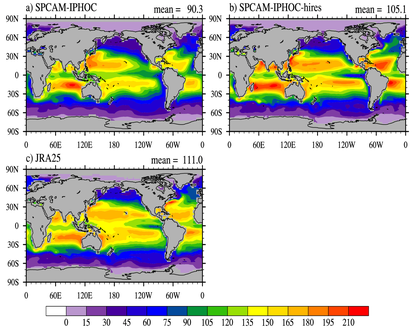

Fig. 6. Global-oceanic and annual-mean surface latent heat flux (W m^{-2}) from SPCAM (a), SPCAM-IPHOC-hires (b), JRA25 reanalysis (c, Kazutoshi et al., 2007).

Overall performance

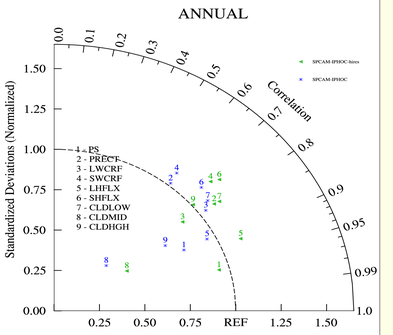

Fig. 7. Taylor diagram for annual-mean variables between 30°S and 30°N for the two experiments, reanalysis data and observations. The reanalysis and observation are denoted by the REF point.